Sasgen, I., Martinec, Z., Bamber, J. (2010): Combined GRACE and InSAR estimate of West Antarctic ice-mass loss. - Journal of Geophysical Research, 115, F04010

DOI: 10.1029/2009JF001525

Combined GRACE and InSAR estimate of West Antarctic ice mass loss

I. Sasgen,[1] Z. Martinec,[2] and J. Bamber[3]

Received 9 September 2009; revised 19 December 2009; accepted 7 June 2010; published 20 October 2010.

[1] We estimate the mass balance of eight drainage basins in West Antarctica from the Gravity Recovery and Climate Experiment (GRACE) data (GFZ RL04, GSM Level 2) using a constrained inverse-gravimetric approach. We consider InSAR observations of ice surface velocity as an indication of mass change, assuming that large mass loss occurs in areas of fast glacier flow. From these mass distribution functions we construct forward models of the geoid height change and their spatial correlations for each drainage basin. Then the difference between the GRACE data and the forward model is minimized by adjusting the total amount of mass change within each drainage basin. To overcome the ambiguity inherent in this inverse problem, we constrain its solution by including a priori estimates based on the InSAR mass-budget method. However, unconstrained (GRACE only) mass-change estimates can be recovered for three to four combined drainage basins. Differences between GRACE and InSAR values exist mainly for the Pine Island Glacier and Getz Ice Shelf region, resulting in a lower unconstrained GRACE total of −91.0 ± 3.5 Gt/yr (for the years 2002–2008) compared to the InSAR estimate of −116.6 ± 19.0 Gt/yr (outflow measurement for the years 1992, 1996, and 2006). There is evidence that this difference arises from anomalously large accumulation within the GRACE time interval (August 2002 to August 2008) in the Amundsen Sea sector and possibly from an overestimation of ice thickness for parts of the Bellinghausen Sea sector underlying the InSAR mass-budget values.

Citation: Sasgen, I., Z. Martinec, and J. Bamber (2010), Combined GRACE and InSAR estimate of West Antarctic ice mass loss, *J. Geophys. Res.*, *115*, F04010, doi:10.1029/2009JF001525.

1. Introduction

[2] The West Antarctic Ice Sheet mostly rests on bedrock below present-day sea level and it is therefore considered to be rather unstable with regard to perturbations caused by changing climate conditions [e.g., *Lemke et al.*, 2007]. Its potential contribution to global sea level change being ~3.3 m [*Bamber et al.*, 2009]. At present, the most prominent changes, such as rapid thinning and fast glacier flow, are observed mainly on glaciers and ice streams discharging into the Amundsen Sea Embayment, and, to a lesser extent, for glaciers farther west along the coast toward the Wrigley Gulf. In these regions, laser and radar altimetry show decreasing ice surface elevations [e.g., *Davis et al.*, 2005]. With Interferometric Synthetic Aperture Radar (InSAR), exceptionally high ice surface velocities of up to ~3 km/yr are observed, which are in some parts increasing [e.g., *Thomas et al.*, 2004; *Rignot*, 2008]. Satellite gravimetry data from the Gravity Recovery and Climate Experiment (GRACE) [e.g., *Tapley et al.*, 2004a, 2004b; *Tapley and Reigber*, 2001] recently confirmed that the most prominent net losses of ice mass in Antarctica are located in the Amundsen Sea sector [e.g., *Ramillien et al.*, 2006; *Horwath and Dietrich*, 2009].

[3] The GRACE mission consists of two satellites flying in near-polar orbits at an altitude of ~450 km. The spacecrafts are separated by ~200 km and continuously measure their distance with a microwave link at μm accuracy. This measurement, together with onboard accelerometer measurements of nongravitational forces, and star cameras and GPS data of the satellites' orientation and position, respectively, allows the determination of the Earth's gravity field with unprecedented accuracy at monthly time intervals [e.g., *Schmidt et al.*, 2008]. The time series of GRACE gravity fields can be inverted for mass changes in the Earth's interior and on its surface, e.g., to constrain the glacial-isostatic adjustment (GIA) of the Earth caused by the retreat of the late-Pleistocene ice sheets, [e.g., *Tamisiea et al.*, 2007; *Sasgen et al.*, 2007b; *Paulson et al.*, 2007], and to determine the mass balance of the major contemporary ice sheets [e.g., *Velicogna and Wahr*, 2006, 2005]. The principal problem of the gravity field inversion is its instability and nonuniqueness, which may lead to ambiguous and

[1]Department of Geodesy and Remote Sensing, GeoForschungsZentrum Potsdam, Potsdam, Germany.
[2]School of Theoretical Physics, Dublin Institute for Advanced Studies, Dublin, Ireland.
[3]School of Geographical Sciences, University of Bristol, Bristol, UK.

0148-0227/10/2009JF001525

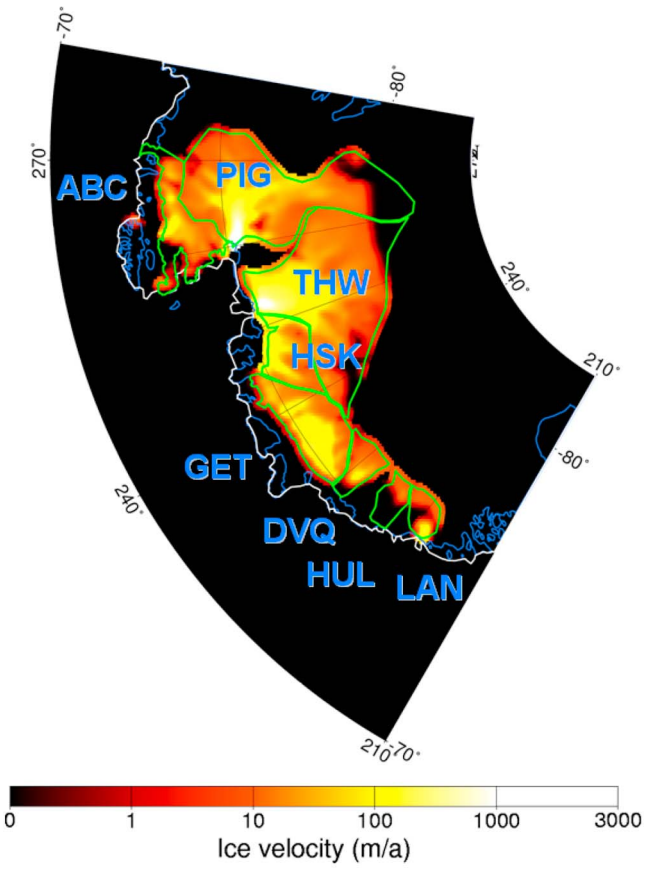

Figure 1. Ice surface velocity in the Amundsen Sea sector from InSAR [*Edwards*, 2009]. The drainage basins (green outlined) are Abbot and Cosgrove (ABC), Pine Island Glacier (PIG), Thwaites (THW), Haynes/Smith/Kohler (HSK), Getz (GET), DeVicq(DVQ), Hull (HUL), and Land (LAN).

unrealistic results, particularly when considering small spatial scales. The instability of the inverse solution can be overcome by limiting the resolution of GRACE data with spatial smoothing filters typically of ~400 km [e.g., *Jekeli*, 1981; *Wahr et al.*, 1998] that optimize the trade-off between resolution and noise [e.g., *Sasgen et al.*, 2006; *Schrama and Visser*, 2007]. The nonuniqueness can be handled by introducing geophysical a priori constraints stabilizing the inverse solution.

[4] In this paper, we determine the mass balances of eight West Antarctic drainage basins from ~6 years of monthly mean GRACE gravity fields. The ambiguity in the mass balance estimates occurring at the spatial resolution of a few hundred km are resolved by constraining the inversion with forward models based on InSAR data, the amount of constraint depending on the uncertainties in the GRACE and InSAR data. This approach allows us to determine the number of drainage basins that are resolvable with GRACE data alone, and we provide the associated mass balance estimates.

2. Observations

2.1. GRACE Data

[5] We use 68 unconstrained GRACE monthly solutions of the Earth's gravity field provided by German Research Centre For Geosciences (GFZ RL04, GSM Level 2 data; http://isdc.gfz-potsdam.de/) [*Flechtner*, 2005]. The time series of Stokes gravitational potential coefficients are complete to degree and order 120 and cover ~6 years, from August 2002 to August 2008. Data gaps within this time interval exist for the months September and December 2002, January and June 2003, as well as January 2004. We fit the time series of each Stokes coefficient by a six-parameter model consisting of an annual and semiannual oscillating component of 365.24 days and 182.62 days, respectively, a linear trend and an offset by the method of least squares assuming calibrated GRACE errors [*Schmidt et al.*, 2008].

[6] During decomposition, and throughout this paper, three models of variances of GRACE coefficients are used: formal and calibrated (F. Flechtner, Release notes for GFZ RL04 GRACE L2 products, 2010), as well as residual, the latter being an empirical estimate based on the residuals after removing deterministic signal components in the Stokes coefficients' time series. No additional filtering or smoothing is applied. Instead, we repeat the inversion for increasing spherical-harmonic cutoff degrees such that increasing noise in the GRACE coefficients propagates to the resulting mass change estimate. Uncertainties at high latitudes are significantly below the global average due to denser track coverage [e.g., *Schmidt et al.*, 2008] and show less striping, particularly for the temporal trend [*Davis et al.*, 2008]. To retain these regional noise characteristics, we refrain from applying a priori smoothing or decorrelation filtering as proposed by *Swenson and Wahr* [2006].

2.2. InSAR Data

[7] We consider ice surface velocities from InSAR (Figure 1) as an indication of the spatial distribution of mass changes in the Amundsen Sea sector [*Edwards*, 2009]. The InSAR data covers nearly all of the drainage basins flowing into Abbot and Cosgrove ice shelves (ABC), as well as those in the Amundsen Sea sector, i.e., Pine Island Glacier (PIG), Thwaites (THW), Haynes/Smith/Kohler (HSK), Getz (GET) and DeVicq (DVQ). Hull (HUL) and Land (LAN) are not completely covered by this InSAR data set and their values are substituted by modeled balance velocities [*Bamber et al.*, 2000]. In addition, we adopt the mass-budget estimates for the individual drainage basins from *Rignot et al.* [2008] for time epochs as close as possible to the midpoint of the GRACE observation period (Tables 1 and 2); this includes an unpublished update for the year 2006 of the mass budget of PIG, THW and HSK. The values represent the difference between average accumulation (input) for the years 1980 to 2004 obtained from regional atmospheric climate modeling for Antarctica (RACMO2/ANT) [*van den Broeke et al.*, 2006a; *van de Berg et al.*, 2006; *van den Broeke et al.*, 2006b], and outflow, which is calculated from the InSAR measured ice flow velocity over the grounding line for the years 1992 (ABC), 1996 (GET, DVQ, HUL and LAN) and 2006 (PIG, THW and HSK). The main error of the mass-budget values arises from uncertainties in the accumulation (input) estimate and determining ice thickness at the fluxgate. It amounts to ~10% for low-accumulation, large basins, and to ~30% for high-accumulation and small basins in the vicinity of the

Table 1. Ice Mass Change for Four Combined Drainage Basins in the Amundsen Sea Sector[a]

Drainage Basin	Area (10^3 km^2)	Year	InSAR		GRACE	
			m (Gt/yr)	σ (Gt/yr)	$\tilde{m}_u$ (Gt/yr)	$\tilde{\sigma}_u$ (Gt/yr)
ABC/PIG	191.5	1992/2006	−53.9	13.8	−28.3	1.3
THW/HSK	218.4	2006	−45.0	14.0	−43.2	1.8
GET	92.1	1996	−11.1	18.3	−4.5	2.2
DVQ/HUL/LAN	43.0	1996	−21.6	3.5	−15.0	1.7
Total	517.5		−116.6	19.0	−91.0	3.5

[a]For the InSAR data, the year of the outflow measurement is indicated. The GRACE data (GFZ RL04) is based on the time interval August 2002 to August 2008, calibrated GRACE errors, and cutoff degrees $j_{min} = 7$ and $j_{max} = 55$, with the GIA correction HUY applied (see text).

coast; outflow uncertainties lie between 2 to 15% [*Rignot et al.*, 2008].

3. GIA Correction

[8] We subtract the trend in the gravity field caused by GIA in Antarctica, y^{GIA}, from the GRACE observation, y^{GRACE} (Figure 2). GIA is modeled using the viscoelastic earth model of *Martinec* [2000] consisting of an elastic lithosphere of thickness 100 km, an upper mantle of viscosity 5.2×10^{20} Pa s, a lower mantle of viscosity 5.9×10^{21} Pa s and a fluid core. The earth model is subjected to the glacial history of the Antarctic Ice Sheet for the last 120 kyr based on the thermomechanical ice sheet model of *Huybrechts* [2002, hereafter HUY]. Following *Sasgen et al.* [2007b], HUY was adjusted to an Antarctic contribution to sea level change since Last Glacial Maximum (LGM) of 9 m, such that the predicted GIA amplitude over the Ronne Ice Shelf, which is the Antarctic region where the largest GIA amplitude is expected (rate of geoid height change of ~1.5 mm/yr), agrees with the GRACE observations for the viscosity structure specified above. Over the Amundsen Sea sector, GIA due to HUY is less important (rate of geoid height change <1 mm/yr). Similar amplitudes are also obtained using the geomorphologic reconstruction of *Lambeck and Chappell* [2001, hereafter ANU]. Regional details of Paleocene and Holocene ice retreat in the Amundsen Sea sector that may have induced a local GIA signal are not sufficiently well known to be included in this modeling. Instead, we instigate the differences arising from correcting with deglaciation scenarios HUY and ANU, and without applying a GIA correction. The Antarctic component of ICE-5G [*Peltier*, 2004], which is a scaled version of the one included in ICE-3G [*Tushingham and Peltier*, 1991], is not investigated, because the model predicts the largest GIA signal over the Ross Ice Shelf, which is not supported by the GRACE data [*Sasgen et al.*, 2007b] or the recent geomorphologic reconstruction of the Antarctic glacial history, IJ05 [*Ivins and James*, 2005]. In the following, the GIA corrected trend in the GRACE gravity fields (Figure 2) is denoted as

$$y(\mathbf{\Omega}) = y^{GRACE}(\mathbf{\Omega}) - y^{GIA}(\mathbf{\Omega}), \quad (1)$$

where $\mathbf{\Omega}$: = (ϑ, φ) stands for the spherical colatitude ϑ and longitude φ.

4. Forward Modeling of Gravity-Field Changes

[9] We model the trend in the gravity field arising from mass changes in k = 1, 2, …, 8 drainage basins in the Amundsen Sea sector (ABC, PIG, THW, HSK, GET, DVQ, HUL and LAN) (Figure 1) by allocating their total mass change, $\mathbf{m} = \{m_k\}_{k=1,2,\ldots,8}$, according to the spatial mass distribution function $\mathbf{w}(\mathbf{\Omega})$. Inside each basin, $w_k(\mathbf{\Omega})$ is linearly proportional to the ice surface velocity from InSAR (Figure 1), outside the basin $w_k(\mathbf{\Omega}) = 0$. The underlying assumption is that mass loss in the Amundsen Sea sector predominantly occurs in areas of fast glacier flow, which is supported by empirical and theoretical evidence [*Rignot et al.*, 2008]. For mass conservation, $w_k(\mathbf{\Omega})$ can be compensated by a water layer uniformly distributed over the area of today's ocean. However, its effect on the results is negligible for this regional investigation and it is therefore not considered in the following derivation.

[10] We normalize the spatial mass distribution function according to $\int_{\Omega_0} w_k(\mathbf{\Omega}) d\mathbf{\Omega} = 1$ for all k and expand it to fully normalized spherical harmonics of degree j andorder m, $Y_{jm}(\mathbf{\Omega})$, where $\mathbf{w}(\mathbf{\Omega}) = \sum_{j=0}^{\infty} \sum_{m=-j}^{m=j} \mathbf{w}_{jm} Y_{jm}(\mathbf{\Omega})$. Then, for each drainage basin, the normalized geoid height change $\mathbf{x}(\mathbf{\Omega}) = \{x_k(\mathbf{\Omega})\}_{k=1,2,\ldots,8}$ is calculated by

$$x_k(\mathbf{\Omega}) = \frac{4\pi G R}{g_0} \sum_{j=j_{min}}^{j_{max}} \frac{(1+q_j)}{2j+1} \sum_{m=-j}^{j} w_{jm}^k Y_{jm}(\mathbf{\Omega}), \quad (2)$$

where G is the gravitational constant, R is the radius of the Earth, g_0 the gravity at the Earth's surface, j_{min} and j_{max} are the lower and upper cutoff degree of the spherical harmonic expansion series, respectively, and q_j are the elastic-compressible surface-load Love numbers [e.g., *Farrell*, 1972; *Wahr et al.*, 1998; *Han and Wahr*, 1995]. Throughout this study, we apply the lower cutoff degree of $j_{min} = 7$ to reduce

Table 2. Ice Mass Change for Eight Drainage Basins in the Amundsen Sea Sector[a]

Drainage Basin	Area (10^3 km^2)	Year	InSAR		GRACE + InSAR	
			m (Gt/yr)	σ (Gt/yr)	$\tilde{m}_c$ (Gt/yr)	$\tilde{\sigma}_c$ (Gt/yr)
ABC	27.5	1992	−14.9	9.1	−9.2	1.3
PIG	164.0	2006	−39.0	10.3	−20.3	1.4
THW	181.9	2006	−26.0	12.9	−21.5	1.2
HSK	36.5	2006	−19.0	7.1	−23.2	0.8
GET	92.1	1996	−11.1	18.3	−1.1	1.3
DVQ	16.0	1996	−14.0	4.7	−9.5	0.7
HUL	14.2	1996	−3.7	1.5	−3.5	0.3
LAN	12.8	1996	−3.9	1.5	−5.3	0.2
Total	517.5		−116.6	19.0	−93.5	2.9

[a]For InSAR data, the year of the outflow measurement is indicated. The GRACE data (GFZ RL04) is based on the time interval August 2002 to August 2008, calibrated GRACE errors, and cutoff degrees $j_{min} = 7$ and $j_{max} = 55$, with the GIA correction HUY applied (see text).

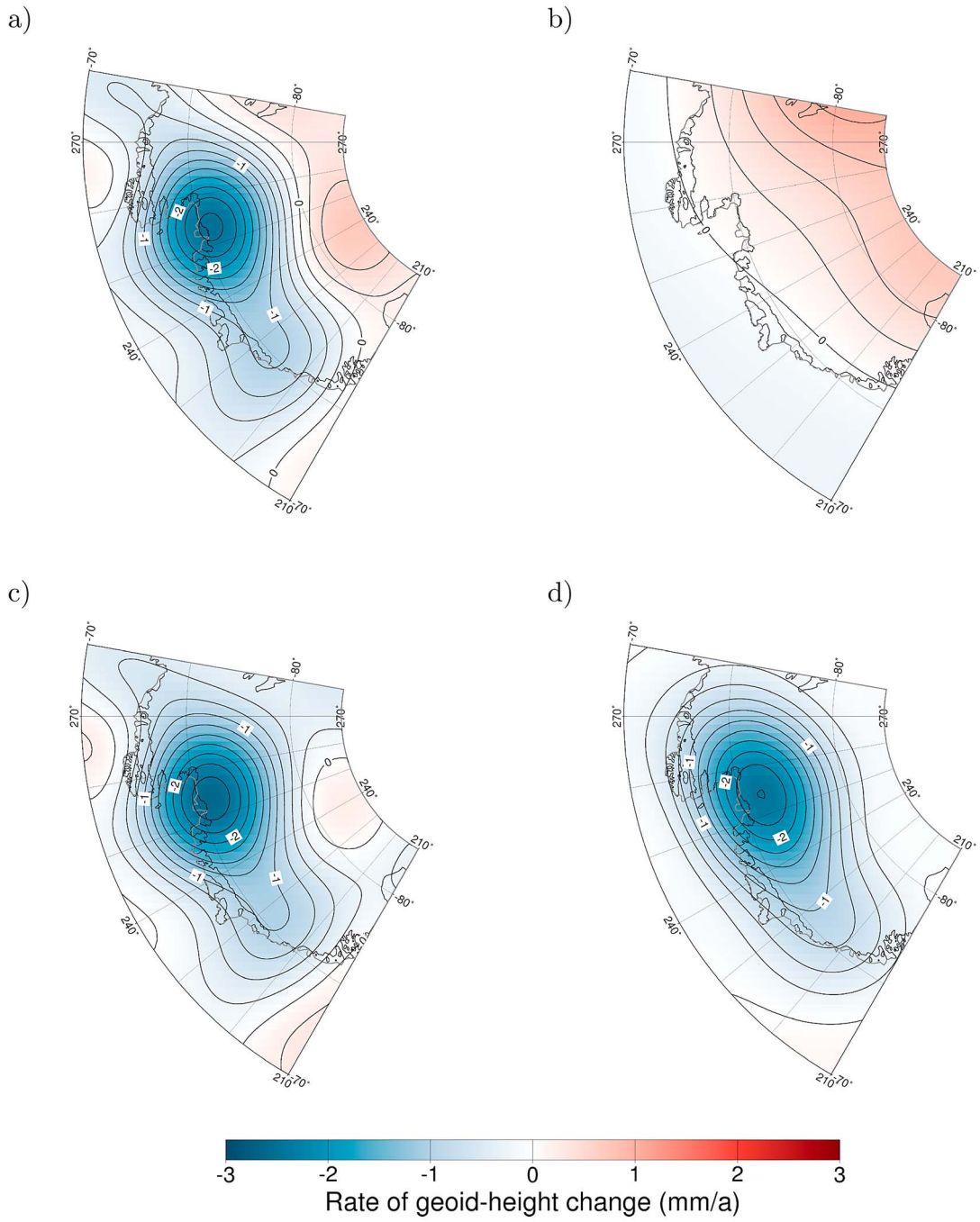

Figure 2. Predicted and observed rate of geoid height change over West Antarctica for (a) GFZ RL04 (without GIA correction), (b) GIA correction, (c) GFZ RL04 minus GIA correction, and (d) optimal forward model based on combined InSAR and GRACE data. The cutoff degrees are $j_{min} = 7$ and $j_{max} = 55$. The time interval of the GRACE data is August 2002 to August 2008.

the influence of far-field signal with respect to Antarctica, which is contained in the low spectral part of the GRACE data. This limit is determined by the degree correlation analysis of the forward modeled geoid height signal for Antarctica and the GRACE data [*Sasgen et al.*, 2007a], which indicates that the long spatial wavelengths of the model and the GRACE data do not significantly correlate for $j_{min} < 7$, and hence, should not be considered for this regional investigation. This procedure also reduces to some extent the influence of the long-wavelength components of the Antarctic GIA signal.

[11] Multiplication of each drainage basin's normalized geoid height change signal $x_k(\Omega)$ with its total mass change m_k and subsequent superposition of signals results in the

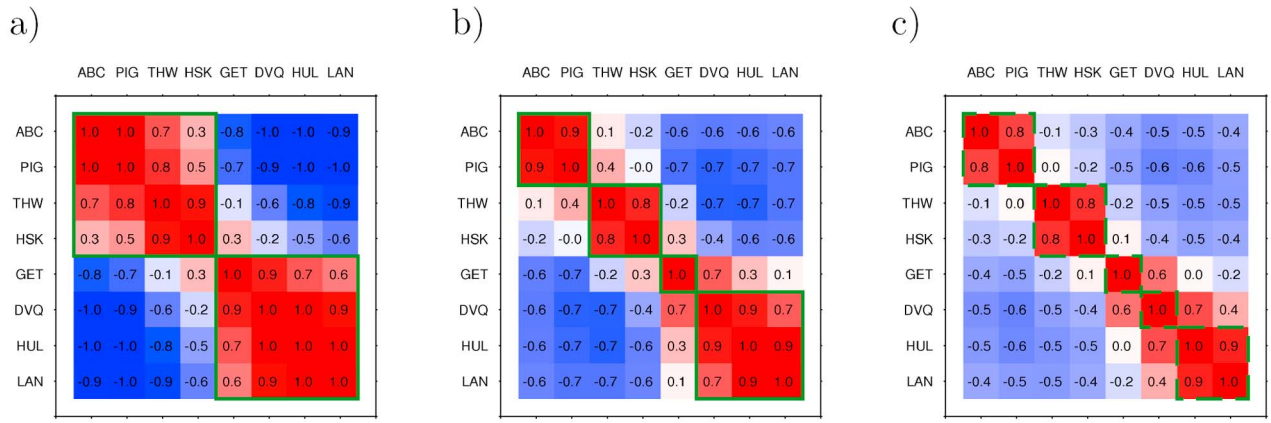

Figure 3. Correlation of model parameters for cutoff degrees $j_{\min} = 7$ and (a) $j_{\max} = 30$, (b) $j_{\max} = 55$, and (c) $j_{\max} = 80$.

forward gravity-field model for the entire Amundsen Sea sector (Figure 2),

$$y^{\mathrm{P}}(\mathbf{\Omega}) = \sum_k x_k(\mathbf{\Omega}) m_k. \tag{3}$$

Table 1 lists the InSAR based mass-budget estimates, $\mathbf{m}$, along with their uncertainties $\sigma = \{\sigma_k\}_{k=1,2,\ldots,8}$. The uncertainties in the mass budget were determined from the root-mean-square error estimates for the different inputs in the calculation. These are accumulation averaged over the catchment, surface velocity and ice thickness at the grounding line. The errors for each input varied depending on the source of the estimate and spatial constraints on accuracy such as local topographic conditions, gradient in accumulation and proximity to in situ observations [*Rignot et al.*, 2008]. As a consequence, the forward model's uncertainties are described by the a priori covariance matrix, $\mathbf{C}_{\mathrm{M}} = \gamma_{kl}\sigma_k\sigma_l$, where γ_{kl} is the spatial correlation [e.g., *Gubbins*, 2004] between the drainage basin signals of geoid height change, γ_{kl} : = corr $(x_k(\mathbf{\Omega}), x_l(\mathbf{\Omega}))$. These correlations are caused by overlapping of the individual gravity field signals, which are spatially smoothed signals compared to the initial mass distributions.

[12] Figure 3 shows the correlations of the forward models γ_{kl} of the eight drainage basins ordered according to their geographical proximity for upper spherical-harmonic cutoff degrees $j_{\max} = 30$, 55 and 80. Increasing the cutoff degree reduces correlations between signals. At cutoff degree $j_{\max} = 30$, the correlation matrix shows two distinct blocks (green outline in Figure 3), consisting of the drainage basins ABC, PIG, THW, HSK, and the drainage basins GET, DVQ, HUL and LAN, respectively. This suggests that mass changes derived from the gravity field can be retrieved for these regions independently. At cutoff degree $j_{\max} = 55$, combined signals from four regions are resolvable. However, even at cutoff degree $j_{\max} = 80$, significant overlaps between the eight drainage basin signals exist, which may lead to ambiguous and unrealistic results of the gravity-field inversion.

5. Inversion of the Gravity-Field Changes

[13] We aim to find a mass change distribution in the Amundsen Sea sector, such that $\|y(\mathbf{\Omega}) - y^{\mathrm{P}}(\mathbf{\Omega})\|$ is minimized, where $y(\mathbf{\Omega})$ is the GRACE observation in equation (1) and $y^{P}(\mathbf{\Omega})$ is the forward gravity model in equation (3). We formulate this inverse problem in terms of the design matrix $\mathbf{F}$, which consists of the normalized geoid height change arising from the kth drainage basin at the ith spatial grid point, $\mathbf{\Omega}_i$, $i = 1, 2, \ldots, N$ (here, a 0.25° × 0.25° grid), $\mathbf{F} = \{x_k(\mathbf{\Omega}_i)\}_{i=1,2,\ldots,N}^{k=1,2,\ldots,8}$. Then, the spatially gridded forward model is expressed by $\mathbf{y}^{\mathrm{P}} = \{y^{\mathrm{P}}(\mathbf{\Omega}_i)\}_{i=1,2,\ldots,N} = \mathbf{Fm}$ and the L_2-norm minimization criterion is such that the squared difference between $\mathbf{y}$ and $\mathbf{y}^{\mathrm{P}}$ is minimized.

[14] The inversion of GRACE data for mass changes is in principle nonunique and unstable, due to the limited resolution of the GRACE data and the smoothing (integral) property of the gravity field measured, which is visible from equation (2). In general, the system of equations resulting from the minimization criterion is possibly underdetermined and it may be necessary to stabilize their solution by including a priori constraints on the parameterized total mass change, $\mathbf{m}$, and their uncertainties, σ. This constrained solution is given by [e.g., *Gubbins*, 2004; *Tarantola*, 2005]

$$\tilde{\mathbf{m}}_{\mathrm{c}} = \mathbf{m} + \left(\mathbf{F}^{\mathrm{T}}\mathbf{C}_{\mathrm{D}}^{-1}\mathbf{F} + \mathbf{C}_{\mathrm{M}}^{-1}\right)^{-1}\mathbf{F}^{\mathrm{T}}\mathbf{C}_{\mathrm{D}}(\mathbf{y} - \mathbf{Fm}), \tag{4}$$

where $\mathbf{C}_{\mathrm{D}}$ and $\mathbf{C}_{\mathrm{M}}$ are the variance-covariance matrices of the GRACE data and the forward model, respectively, and T denotes matrix transposition.

[15] The amount of a priori information included in the inversion is governed by the balance between data and model variances. It can be quantified by the resolution matrix, $\mathbf{R} = \mathbf{I} - \tilde{\mathbf{C}}_{\mathrm{M}}\mathbf{C}_{\mathrm{M}}^{-1}$, where $\tilde{\mathbf{C}}_{\mathrm{M}}$ represents the a posteriori parameter covariances of the GRACE+InSAR model given by $\tilde{\mathbf{C}}_{\mathrm{M}} = (\mathbf{F}^{\mathrm{T}}\mathbf{C}_{\mathrm{D}}^{-1}\,\mathbf{F} + \mathbf{C}_{\mathrm{M}}^{-1})^{-1}$ [e.g., *Gubbins*, 2004; *Tarantola*, 2005]. The trace of the resolution matrix, $tr\mathbf{R}$, can be interpreted as the number of parameters resolved by the data (here, the GRACE data),

$$tr\mathbf{R} = tr\mathbf{I} - tr\left(\tilde{\mathbf{C}}_{\mathrm{M}}\mathbf{C}_{\mathrm{M}}^{-1}\right), \tag{5}$$

whereas $tr\mathbf{I}$ and $tr(\tilde{\mathbf{C}}_{\mathrm{M}}\mathbf{C}_{\mathrm{M}}^{-1})$ are the total number of parameters (here, eight drainage basins) and the number of parameters constituted by a priori information (here, the InSAR model), respectively.

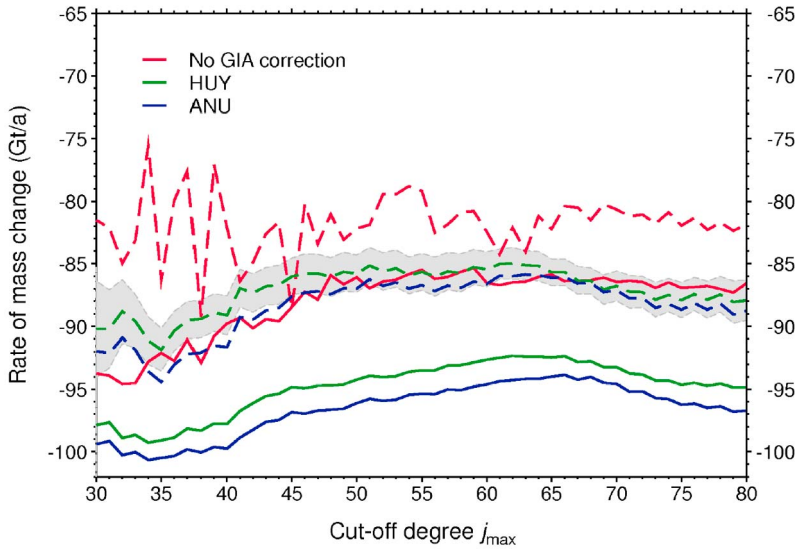

Figure 4. Mass change in the Amundsen Sea sector obtained by constrained (solid) and unconstrained (dashed) inversion of GRACE gravity fields without GIA correction (red), as well as with GIA corrections based on HUY (green), minimum/maximum HUY (grey shaded area, unconstrained solution), and ANU (blue) for cutoff degrees $j_{max} = 30$ to $j_{max} = 80$.

[16] The spatial representation of the GRACE variances, $\mathbf{C}_{GRACE}$, is calculated according to

$$\mathbf{C}_D = \{\mathrm{var}(y)\}_{i_1=1,2,\ldots,N}^{i_2=1,2,\ldots,N} = \sum_{jm} Y_{jm}(\mathbf{\Omega}_{i_1})\mathrm{var}(y_{jm})Y_{jm}^{*}(\mathbf{\Omega}_{i_2}) \quad (6)$$

for formal, calibrated and residual variances of the linear trend in the Stokes potential coefficients, var(y_{jm}), which are considered to be statistically independent.

6. Results

6.1. Influence of Cutoff Degree and GIA Correction on the Total Mass-Change Estimate

[17] Figure 4 shows the total mass change in the Amundsen Sea sector, $\sum_{k=1}^{8} \tilde{m}_k$, for the unconstrained (GRACE, dashed) and constrained (i.e., GRACE+InSAR, solid) inversion. Without GIA correction (red) unconstrained mass change estimates exhibit large variations for cutoff degrees $j_{max} \leq 45$. With GIA correction (green for HUY and blue for ANU) this sensitivity is reduced and, in addition, resulting mass changes estimates are largely constant for cutoff degrees $j_{max} > 45$. This suggests that removing the GIA prediction from the GRACE data improves the consistency between data and forward model. Since the GIA signal is mainly constituted of long spatial wavelengths, results are more sensitive to the GIA correction for the low spectral range and the decrease in mass loss between $j_{max} = 30$ and 45 indicates remaining deficiencies, i.e., an overestimation, of the GIA prediction.

[18] For cutoff degrees $j_{max} = 45$ to 80, the unconstrained mass loss ranges between −84 and −89 Gt/yr, when correcting with the minimum and maximum GIA prediction for HUY (grey shaded area). This GIA uncertainty estimate also encompasses values obtained when using the ANU model, as well as when employing the glacial history of HUY and varying the upper- and lower-mantle viscosities between 4×10^{20} and 8×10^{20} Pa s, and 5×10^{21} and 4×10^{22} Pa s. Constraining the inversion with InSAR mass-budget estimates according to equation (4) leads to more negative mass loss rates between ∼−92 and −95 Gt/yr (HUY) and ∼−94 and −97 Gt/yr (ANU), which are closer to the InSAR estimate of ∼−116.6 ± 19.0 Gt/yr based on ice surface velocity data from the years 1992 (ABC), 1996 (GET, DVQ, HUL and LAN) and 2006 (PIG, THW, HSK) (Table 1). Although the superposed signals of all eight unconstrained mass change estimates fulfill the minimization criterion and result in a plausible total mass changes estimate, the individual values are likely not to be geophysically meaningful. As a consequence, we will now reduce the eight drainage basins to a number resolvable by GRACE and accordingly refine the total mass change estimate presented in this sensitivity analysis.

6.2. Resolvability of Individual Drainage Basins

[19] Figure 5 shows the number of parameterized drainage basins resolved by the GRACE data for cutoff degrees $j_{max} = 10$ to 80, which is calculated according to equation (5). For calibrated GRACE uncertainties (green), the number of drainage basins resolved increases from around two at cutoff degree $j_{max} = 20$ to a maximum of around four at degree 55 and remains largely constant until degree 80; at cutoff degree $j_{max} \approx 55$, GRACE and InSAR constitute approximately four drainage basins each, meaning that both data sets are combined in the inversion with approximately equal weights. With the more pessimistic residual GRACE uncertainties (blue), a cutoff degree of $j_{max} \approx 65$ is necessary to resolve four drainage basins. For formal GRACE uncertainties (red), which are currently too optimistic, but result from the formal error propagation associated with the determination of the Stokes coefficients, at most five drainage basins can be resolved.

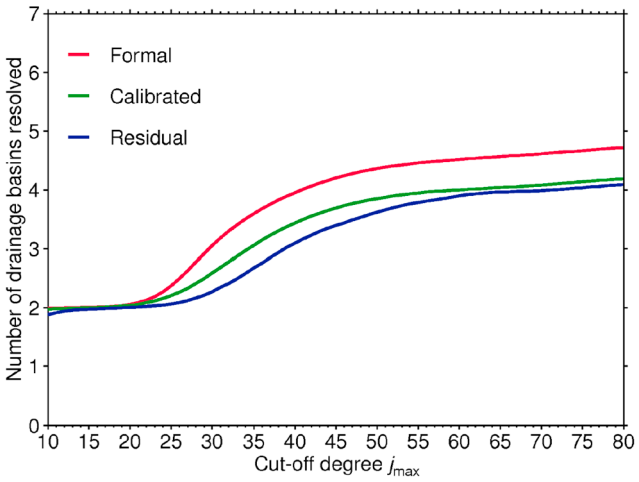

Figure 5. Number of parameters resolved by GRACE for cutoff degrees $j_{max} = 30$ to $j_{max} = 80$ considering formal, calibrated, and residual GRACE uncertainties.

6.3. Mass Change for Four Combined Drainage Basins

[20] We now combine the eight drainage basins to four to account for the expected GRACE resolution for calibrated uncertainties (Figure 5). This is done by merging drainage basins with high signal correlations γ_{kl} in the forward model (Figure 3),i.e., ABC/PIG, THW/HSK, GET and HUL/DVQ/LAN. For the reduced number of parameters (i.e., $k \lesssim tr\mathbf{R}$), the unconstrained solution of the inverse problem, $\tilde{\mathbf{m}}_u = (\mathbf{F}^T\mathbf{C}_D^{-1}\mathbf{F})^{-1}\ \mathbf{F}^T\mathbf{C}_D\mathbf{y}$, is approximately equal to the constrained solution equation (4) (not shown here).

[21] Table 1 lists the mass balance of the four merged drainage basins from InSAR [*Rignot et al.*, 2008] and GRACE for cutoff degree $j_{max} = 55$. Uncertainties are calculated according to $\tilde{\sigma}_{clu} = \sqrt{\mathrm{diag}(\tilde{\mathbf{C}}_M)}$. The unconstrained GRACE estimates compare well with the InSAR estimate for THW/HSK (for the year 2006) and for HUL/DVQ/LAN (for the year 1996). For GET, InSAR indicates (with large uncertainties) a mass loss of −11.1 ± 18.3 Gt/yr for the year 1996, whereas GRACE recovers ∼−4.5 ± 2.2 Gt/yr. Also, for the combined ABC/PIG basin GRACE does not support mass loss in excess of ∼30 Gt/yr opposed to the InSAR (−53.9 ± 13.8 Gt/yr for the years 1996/2006, respectively). In sum, GRACE gives 22% less negative values for the entire Amundsen Sea sector than the InSAR mass-budget method.

6.4. Mass Change for Eight Drainage Basins

[22] The resolution diagram (Figure 5) indicates that recovering independent signals from all eight drainage basins from GRACE data alone is not possible, and the inversion needs to be stabilized with the InSAR estimates. Table 2 shows that differences between GRACE+InSAR and InSAR estimates are below ∼5 Gt/yr for all drainage basins. Exceptions are GET, for which the combined estimate of −1.1 ± 1.3 Gt/yr lies ∼10 Gt/yr below the InSAR value, and PIG, for which the GRACE+InSAR estimate of −20.3 ± 1.4 Gt/yr is nearly half of the InSAR value (−39.0 ± 10.3 Gt/yr).

6.5. Robustness of the Results With Respect the GRACE Release

[23] Data sets of GRACE gravity fields from various GRACE processing centers may show significant differences for the individual monthly solutions, as well as for the estimated linear trends. We therefore test the robustness of our results with the respect to the employed GRACE data set, by calculating estimates the CSR RL04 GRACE release (http://isdc.gfz-potsdam.de/) [*Bettadpur*, 2007] using the same months as for the GFZ RL04 estimates the GIA correction. For most of the individual and combineddrainage basins, the mass change estimates agree within ∼2 Gt/yr. Exceptions are the unconstrained estimates for GET and DVQ/HUL/LAN; compared to GFZ RL04, the CSR RL04 indicates stronger mass loss for GET (−9.4 ± 2.2 Gt/yr) and weaker massloss for DVQ/HUL/LAN (−8.2 ± 1.7 Gt/yr), which improves the agreement with the InSAR data for GET, but decreases it for DVQ/HUL/LAN. The difference for the total of the entire Amundsen Sea sector from CSR RL04 and GFZ RL04 is below 1 Gt/yr, and therefore well within the GRACE error bounds.

7. Discussion

[24] The GRACE-estimated total mass loss in the Amundsen Sea sector of −91.0 ± 3.5 Gt/yr (Table 1) largely confirms previous GRACE estimates, e.g., −81.0 ± 17 Gt/yr [*Chen et al.*, 2008] and −88 ± 10 Gt/yr [*Horwath and Dietrich*, 2009], but it is significantly lower than the value of −116.6 ± 19.0 Gt/yr recovered by InSAR, which is, however, not derived for coincident observation periods. Most of this discrepancy is attributed to the drainage basins ABC/PIG and GET (InSAR estimates from the years 1992/2006 and 1996, respectively). The GRACE values may underestimate mass loss if the GIA signal modeled and subtracted from the GRACE data is too low in amplitude, although corrections in excess of an additional ∼−5 Gt/yr are not supported by plausible GIA scenarios (Figure 4). If we include the Ferrigno ice streams and the glaciers flowing into the Venable ice shelf in our forward model, GRACE mass loss further reduces for ABC/PIG by 2 Gt/yr (<1 Gt/yr for other drainage basis) due the removal of signal overlapping (leakage). Also, the influence of mass trends in the atmosphere and ocean estimated from the GRACE dealiasing product is <2 Gt/yr [*Flechtner*, 2006] and cannot explain the discrepancy between InSAR and GRACE. In addition, InSAR gives clear evidence for an approximate linear increase in outflow of PIG, THW, and HSK from the years 1974 to 2007 [*Rignot*, 2008], which would favor larger mass losses for the later time interval observed GRACE with respect to the InSAR data. For example, PIG was 26%, 39%, 64% and 75% out of balance in the years 1996, 2000, 2006 and 2007, assuming the average accumulation of ∼61 Gt/yr for the years 1980 to 2004 [*Rignot*, 2008; *Rignot et al.*, 2008]. This should induce a quadratic term in the GRACE time series, and, excluding the latest twelve months of GRACE data reduces mass loss rates of ABC/PIG by ∼6 Gt/yr, but we do not find this accelerating term to be statistically significant. Also, the value of PIG adopted here dates from the year 2006, which is close to the midpoint interval of the GRACE period, and GRACE and

InSAR should reflect trend observations of comparable time epochs.

[25] An overestimation of mass loss by InSAR may be the consequence of larger accumulation within the GRACE time interval (August 2002 to August 2008) compared to the mean of the years 1980 to 2004 from RACMO2/ANT underlying the mass-budget values for ABC/PIG and GET. Interannual variations in accumulation rate with respect to the mean are ~15% [*Shepherd and Wingham*, 2007] and may compensate the drainage basin imbalances caused by increased outflow (~10 to 50%). RACMO2/ANT simulates a positive accumulation anomaly of ~10 Gt/yr for the Amundsen Sea Embayment for the time interval 1995 to 2003 with respect to the 1980–2004 mean, which possibly persisted for the GRACE observation period. It should also be noted that the terrain of the drainage basins ABC and PIG is complex and the floating tongue, used to estimate ice thickness for the InSAR outflow calculation, narrow. As a consequence uncertainties in the InSAR derived estimates of mass balance in this area may be larger than assumed, and outflow may be overestimated. An overestimation by InSAR is supported by the lack of thinning observed the satellite radar altimetry between the years 1995 and 2005 [*Rignot et al.*, 2008].

8. Conclusion

[26] We have performed a joint inversion of GRACE gravity fields from August 2002 to August 2008 and InSAR data (years of outflow measurement 1992, 1996 and 2006) to determine the mass balances of eight West Antarctic drainage basins. Depending on the GRACE errors approximately three to five combined drainage basins can be resolved by GRACE data alone. For the reduced number of four combined drainage basins, values from InSAR and GRACE agree within ~±5 Gt/yr for the drainage basins THW/HSK and HUL/DVQ/LAN (Figure 1 and Table 1). However, GRACE cannot confirm the large mass losses for ABC/PIG (−53.9 ± 13.8) and GET (−11.1 ± 18.3) inferred from InSAR. Mainly these deviations are responsible for a GRACE total of −91.0 ± 3.5 Gt/yr(years 2002 to 2008), which is, despite being in agreement with previous GRACE estimates [*Chen et al.*, 2008; *Horwath and Dietrich*, 2009], ~26 Gt/yr lower than the values derived from InSAR (outflow measurements for the years 1992, 1996 and 2006). The discrepancy can neither be reconciled by modifying the GIA correction applied to the GRACE data, nor can it be explained by signal leakage from the atmosphere and the ocean or neighboring drainage basins, and it should therefore result from the nonstationarity of the ice mass signals at interannual timescales. We suggest that this difference is caused by anomalously large accumulation within the GRACE time interval (August 2002 to August 2008) compared to the mean of the years 1980 to 2004 underlying the InSAR mass-budget estimate [*Helsen et al.*, 2008]. An additional contribution to increased InSAR-determined mass loss may arise from larger than expected errors in ice thickness estimation due to a complex terrain in parts of the Bellinghausen Sea sector.

[27] **Acknowledgments.** We thank two anonymous reviewers for their comments that have helped to improve the manuscript. I.S. acknowledges support from the Deutsche Forschungsgemeinschaft (DFG) (German Research Foundation) through grant MA 3432/3-1 (SPP1257) and is grateful to Erik Ivins for his comments on the manuscript. Z.M. acknowledges support from the Grant Agency of the Czech Republic through Grant 205/09/0546. J.L.B. is grateful to Ron Kwok, JPL and Ian Joughin, and APL for providing their unpublished InSAR data and to Laura Edwards for combining these with other InSAR data. J.L.B. was partially funded by U.K. Natural Environment Research Council grant NE/E004032/1 and a Colorado University Cooperative Institute for Research in Environmental Sciences (CIRES) fellowship.

References

Bamber, J. L., D. G. Vaughan, and I. Joughin (2000), Widespread complex flow in the interior of the Antarctic Ice Sheet, *Science*, *287*(5456), 1248–1250, doi:10.1126/science.287.5456.1248.

Bamber, J. L., R. E. M. Riva, B. L. A. Vermeersen, and A. M. LeBrocq (2009), Reassessment of the potential sea-level rise from a collapse of the West Antarctic Ice Sheet, *Science*, *324*(5929), 901–903, doi:10.1126/science.1169335.

Bettadpur, S. (2007), UTCSR level-2 processing standards document for level-2 product release 0004, *Rep. CSR-GR-03-03*, Univ. of Texas at Austin, Austin, Tex.

Chen, J. L., C. R. Wilson, B. D. Tapley, D. Blankenship, and D. Young (2008), Antarctic regional ice loss rates from GRACE, *Earth Planet. Sci. Lett.*, *266*, 140–148, doi:10.1016/j.epsl.2007.10.057.

Davis, C., Y. Li, J. McConnell, M. Frey, and E. Hanna (2005), Snowfall-driven growth in East Antarctic ice sheet mitigates recent sea-level rise, *Science*, *308*(5730), 1898–1901, doi:10.1126/science.1110662.

Davis, J. L., M. E. Tamisiea, P. Elósegui, J. X. Mitrovica, and E. M. Hill (2008), A statistical filtering approach for Gravity Recovery and Climate Experiment (GRACE) gravity data, *J. Geophys. Res.*, *113*, B04410, doi:10.1029/2007JB005043.

Edwards, L. (2009), Antarctic ice velocities from satellite observations: Generation, validation and application, Ph.D. thesis, Univ. of Bristol, Bristol, U. K.

Farrell, W. E. (1972), Deformation of the earth by surface loads, *Rev. Geophys.*, *10*, 761–797.

Flechtner, F. (2005), GFZ level-2 processing standards document for level-2 product release 0003, *Rep. GRACE 327-743 (GR-GFZ-STD-001)*, GeoForschungsZentrum Potsdam, Wessling, Germany.

Flechtner, F. (2006), AOD1B product description document for product releases 01 to 04, *Rep. GRACE 327-750 (GR-GFZ-AOD-0001)*, GeoForschungsZentrum Potsdam, Wessling, Germany.

Gubbins, D. (2004), *Time Series Analysis and Inverse Theory for Geophysicists*, Cambridge Univ. Press, Cambridge, U. K.

Han, D., and J. Wahr (1995), The viscoelastic relaxation of a realistically stratified earth, and a further analysis of postglacial rebound, *Geophys. J. Int.*, *120*, 287–311.

Helsen, M. M., M. R. van den Broeke, R. S. W. van de Wal, W. J. van de Berg, E. van Meijgaard, C. H. Davis, Y. Li, and I. Goodwin (2008), Elevation changes in Antarctica mainly determined by accumulation variability, *Science*, *320*(5883), 1626–1629, doi:10.1126/science.1153894.

Horwath, M., and R. Dietrich (2009), Signal and error in mass change inferences from GRACE: The case of Antarctica, *Geophys. J. Int.*, *177*, 849–864, doi:10.1111/j.1365-246X.2009.04139.x.

Huybrechts, P. (2002), Sea-level changes at the LGM from ice-dynamic reconstructions of the Greenland and Antarctic ice sheets during the glacial cycles, *Quat. Sci. Rev.*, *21*, 203–231.

Ivins, E. R., and T. S. James (2005), Antarctic glacial isostatic adjustment: A new assessment, *Antarctic Sci.*, *17*(4), 541–553.

Jekeli, C. (1981), Alternative methods to smooth the Earth's gravity field, *Rep. 327*, Dep. of Civ. and Environ. Eng. and Geod. Sci., Ohio State Univ., Columbus, Ohio.

Lambeck, K., and J. Chappell (2001), Sea-level change throughout the last-glacial cycle, *Science*, *292*(5517), 679–686, doi:10.1126/science.1059549.

Lemke, P., et al. (2007), Observations: Changes in snow, ice and frozen ground, in *Climate Change 2007: The Physical Science Basis. Contribution of Working Group I to the Fourth Assessment Report of the Intergovernmental Panel on Climate Change*, edited by S. Solomon et al., pp. 337–383, Cambridge Univ. Press, Cambridge, U. K.

Martinec, Z. (2000), Spectral-finite element approach to three-dimensional viscoelastic relaxation in a spherical earth, *Geophys. J. Int.*, *142*, 117–141.

Paulson, A., S. Zhong, and J. Wahr (2007), Inference of mantle viscosity from GRACE and relative sea level data, *Geophys. J. Int.*, *171*, 497–508, doi:10.1111/j.1365-246X.2007.03556.x.

Peltier, W. R. (2004), Global glacial isostasy and the surface of the ice-age earth: The ICE5G (VM2) model and GRACE, *Ann. Rev. Earth Planet. Sci.*, *32*, 111–149, doi:10.1146/annurev.earth.32.082503.144359.

Ramillien, G., A. Lombard, A. Cazenave, E. R. Ivins, M. Llubes, F. Remy, and R. Biancale (2006), Interannual variations of the mass balance of the Antarctica and Greenland ice sheets from GRACE, *Global Planet. Change*, *53*(3), 198–208, doi:10.1016/j.gloplacha.2006.06.003.

Rignot, E. (2008), Changes in West Antarctic ice stream dynamics observed with ALSO PALSAR data, *Geophys. Res. Lett.*, *35*, L12505, doi:10.1029/2008GL033365.

Rignot, E., J. L. Bamber, M. R. Van Den Broeke, C. Davis, Y. Li, W. J. Van De Berg, and E. Van Meijgaard (2008), Recent Antarctic ice mass loss from radar interferometry and regional climate modelling, *Nat. Geosci.*, *1*(2), 106–110, doi:10.1038/ngeo102.

Sasgen, I., Z. Martinec, and K. Fleming (2006), Wiener optimal filtering of GRACE data, *Stud. Geophys. Geod.*, *50*(4), 499–508.

Sasgen, I., Z. Martinec, and K. Fleming (2007a), Wiener optimal combination and evaluation of the Gravity Recovery and Climate Experiment (GRACE) gravity fields over Antarctica, *J. Geophys. Res.*, *112*, B04401, doi:10.1029/2006JB004605.

Sasgen, I., Z. Martinec, and K. Fleming (2007b), Regional ice-mass changes and glacial-isostatic adjustment in Antarctica from GRACE, *Earth Planet. Sci. Lett.*, *264*, 391–401.

Schmidt, R., F. Flechtner, U. Meyer, K.-H. Neumayer, C. Dahle, R. König, and J. Kusche (2008), Hydrological signals observed by the GRACE satellites, *Surv. Geophys.*, *29*, 319–334, doi:10.1007/s10712-008-9033-3.

Schrama, E. J. O., and P. N. A. M. Visser (2007), Accuracy assessment of the monthly GRACE geoids based upon a simulation, *J. Geod.*, *81*, 67–80, doi:10.1007/s00190-006-0085-1.

Shepherd, A., and D. Wingham (2007), Recent sea-level contributions of the Antarctic and Greenland ice sheets, *Science*, *315*(5818), 1529–1532, doi:10.1126/science.1136776.

Swenson, S., and J. Wahr (2006), Post-processing removal of correlated errors in GRACE data, *Geophys. Res. Lett.*, *33*, L08402, doi:10.1029/2005GL025285.

Tamisiea, M. E., J. X. Mitrovica, and J. L. Davis (2007), GRACE gravity data constrain ancient ice geometries and continental dynamics over Laurentia, *Science*, *316*(5826), 881–883, doi:10.1126/science.1137157.

Tapley, B., and C. Reigber (2001), The GRACE Mission: Status and future plans, *Eos Trans. AGU*, *82*(47), Fall Meet. Suppl., Abstract G41C-02.

Tapley, B., S. Bettadpur, M. Watkins, and C. Reigber (2004a), The gravity recovery and climate experiment: Mission overview and early results, *Geophys. Res. Lett.*, *31*, L09607, doi:10.1029/2004GL019920.

Tapley, B. D., S. Bettadpur, J. C. Ries, P. F. Thompson, and M. M. Watkins (2004b), GRACE measurements of mass variability in the Earth system, *Science*, *305*(5689), 503–505, doi:10.1126/science.1099192.

Tarantola, A. (2005), *Inverse Problem Theory and Methods for Model Parameter Estimation*, Soc. for Ind. and Appl. Math., Philadelphia, Pa.

Thomas, R., et al. (2004), Accelerated sea-level rise from West Antarctica, *Science*, *306*(5694), 255–258, doi:10.1126/science.1099650.

Tushingham, A. M., and W. R. Peltier (1991), ICE-3G: A new global model of late Pleistocene deglaciation based upon geophysical predictions of post-glacial relative sea level change, *J. Geophys. Res.*, *96*, 4497–4523.

van de Berg, W., M. van den Broeke, C. Reijmer, and E. van Meijgaard (2006), Reassessment of the Antarctic surface mass balance using calibrated output of a regional atmospheric climate model, *J. Geophys. Res.*, *111*, D11104, doi:10.1029/2005JD006495.

van den Broeke, M., W. van de Berg, and E. van Meijgaard (2006a), Snowfall in coastal West Antarctica much greater than previously assumed, *Geophys. Res. Lett.*, *33*, L02505, doi:10.1029/2005GL025239.

van den Broeke, M., W. J. van de Berg, E. van Meijgaard, and C. Reijmer (2006b), Identification of Antarctic ablation areas using a regional atmospheric climate model, *J. Geophys. Res.*, *111*, D18110, doi:10.1029/2006JD007127.

Velicogna, I., and J. Wahr (2005), Greenland mass balance from GRACE, *Geophys. Res. Lett.*, *32*, L18505, doi:10.1029/2005GL023955.

Velicogna, I., and J. Wahr (2006), Measurements of time-variable gravity show mass loss in Antarctica, *Science*, *311*(5768), 1754–1756, doi:10.1126/science.1123785.

Wahr, J., M. Molenaar, and F. Bryan (1998), Time variability of the Earth's gravity field: Hydrological and oceanic effects and their possible detection using GRACE, *J. Geophys. Res.*, *103*, 30,205–30,230.

J. Bamber, School of Geographical Sciences, University of Bristol, University Road, Bristol BS8 1SS, UK.

Z. Martinec, School of Theoretical Physics, Dublin Institute for Advanced Studies, 10 Burlington Rd., Dublin 4, Ireland.

I. Sasgen, Department of Geodesy and Remote Sensing, GeoForschungsZentrum Potsdam, Telegrafenberg A20, D-14473 Potsdam, Germany. (sasgen@gfz-potsdam.de)